J|A|C|S
ARTICLES
Published on Web 02/06/2008

Three State Redox-Active Molecular Shuttle That Switches in Solution and on a Surface

Giulia Fioravanti,[‡] Natalia Haraszkiewicz,[||] Euan R. Kay,[†] Sandra M. Mendoza,[§] Carlo Bruno,[‡] Massimo Marcaccio,[‡] Piet G. Wiering,[||] Francesco Paolucci,*[,‡] Petra Rudolf,*[,§] Albert M. Brouwer,*[,||] and David A. Leigh*[,†]

Dipartimento di Chimica "G. Ciamician", Università degli Studi di Bologna, v. F. Selmi 2, 40126, Bologna, Italy, School of Chemistry, University of Edinburgh, The King's Buildings, West Mains Road, Edinburgh EH9 3JJ, United Kingdom, Zernike Institute for Advanced Materials, University of Groningen, Nijenborgh 4, 9747AG Groningen, The Netherlands, and Van't Hoff Institute for Molecular Sciences, University of Amsterdam, Nieuwe Achtergracht 129, NL-1018 WS Amsterdam, The Netherlands

Received September 18, 2007; E-mail: David.Leigh@ed.ac.uk; Francesco.Paolucci@unibo.it; P.Rudolf@rug.nl; A.M.Brouwer@uva.nl

Abstract: Although the desirability of developing synthetic molecular machine systems that can function on surfaces is widely recognized, to date the only well-characterized examples of electrochemically switchable rotaxane-based molecular shuttles which can do so are based on the tetracationic viologen macrocycle pioneered by Stoddart. Here, we report on a [2]rotaxane which features succinamide and naphthalene diimide hydrogen-bonding stations for a benzylic amide macrocycle that can shuttle and switch its net position both in solution and in a monolayer. Three oxidation states of the naphthalene diimide unit can be accessed electrochemically in solution, each one with a different binding affinity for the macrocycle and, hence, corresponding to a different distribution of the rings between the two stations in the molecular shuttle. Cyclic voltammetry experiments show the switching to be both reversible and cyclable and allow quantification of the translational isomer ratios (thermodynamics) and shuttling dynamics (kinetics) for their interconversion in each state. Overall, the binding affinity of the naphthalene diimide station can be changed by 6 orders of magnitude over the three states. Unlike previous electrochemically active amide-based molecular shuttles, the reduction potential of the naphthalene diimide unit is sufficiently positive (−0.68 V) for the process to be compatible with operation in self-assembled monolayers on gold. Incorporating pyridine units into the macrocycle allowed attachment of the shuttles to an acid-terminated self-assembled monolayer of alkane thiols on gold. The molecular shuttle monolayers were characterized by X-ray photoelectron spectroscopy and their electrochemical behavior probed by electrochemical impedance spectroscopy and double-potential step chronoamperometry, which demonstrated that the redox-switched shuttling was maintained in this environment, occurring on the millisecond time scale.

Introduction

Synthetic systems in which submolecular motions can be controlled by the application of external stimuli have been vigorously pursued in recent years.[1] Such "mechanical" molecular devices are viewed both as putative components for future functional nanotechnologies and as much simplified models of complex biological machines. One of the most versatile designs for a simple switch-like molecular machine is the stimuli-responsive molecular shuttle.[1,2] A molecular shuttle is a rotaxane in which the thread contains two (or more) macrocycle-binding sites ("stations") connected by a traversable pathway.[3] Provided sufficient thermal energy is available to break the intercomponent interactions at each site, the ring moves randomly between the two stations. On average, however, the macrocycle spends more time on the station with the higher binding affinity (i.e., the molecule tends to adopt a particular preferred co-conformation[4]). In a stimuli-responsive molecular shuttle, chemically altering one of the stations is used to switch the preferred location of the ring, while reversing that change returns the system to the starting distribution. One particularly attractive stimulus for the operation of such devices is electrochemistry, as it allows remote, reagent-free, and waste-free

[†] University of Edinburgh.
[‡] Università degli Studi di Bologna.
[§] University of Groningen.
[||] University of Amsterdam.

(1) (a) Balzani, V.; Credi, A.; Raymo, F. M.; Stoddart, J. F. *Angew. Chem., Int. Ed.* **2000**, *39*, 3349−3391. (b) Balzani, V.; Venturi, M.; Credi, A. *Molecular Devices and Machines. A Journey into the Nanoworld*; Wiley-VCH: Weinheim, 2003. (c) Kinbara, K.; Aida, T. *Chem. Rev.* **2005**, *105*, 1377−1400. (d) Browne, W. R.; Feringa, B. L. *Nat. Nanotech.* **2006**, *1*, 25−35. (e) Kay, E. R.; Leigh, D. A.; Zerbetto, F. *Angew. Chem., Int. Ed.* **2007**, *46*, 72−191.
(2) Tian, H.; Wang, Q.-C. *Chem. Soc. Rev.* **2006**, *35*, 361−374.
(3) (a) Anelli, P. L.; Spencer, N.; Stoddart, J. F. *J. Am. Chem. Soc.* **1991**, *113*, 5131−5133. For the first example of an amide-based molecular shuttle see: (b) Lane, A. S.; Leigh, D. A.; Murphy, A. *J. Am. Chem. Soc.* **1997**, *119*, 11092−11093.
(4) "Co-conformation" refers to the relative positions of the mechanically interlocked components with respect to each other, see: Fyfe, M. C. T.; Glink, P. T.; Menzer, S.; Stoddart, J. F.; White, A. J. P.; Williams, D. J. *Angew. Chem., Int. Ed. Engl.* **1997**, *36*, 2068−2070.

10.1021/ja077223a CCC: $40.75

control, while providing the opportunity to interface the molecular devices with existing electronic technologies.[5]

Clearly, a key step in the development of electronic (and many other) applications of synthetic molecular machines will be transposing working systems from solution phase onto surfaces and into the solid state.[6] Already molecular shuttles have been used to construct solid-state and surface-based devices that exhibit switchable conductance,[5,7] optical properties,[8] wettability,[9] porosity,[10] and shape.[11] Yet, although stimuli-induced shuttling is strongly implicated in the operation of each of these systems, reliable methods for anchoring shuttles to solid supports and strategies for directly observing and fully characterizing their stimuli-induced motions in such environments have proven particularly challenging over nearly a decade of study.[5−11]

In fact, despite the sophistication of modern synthetic routes toward interlocked molecules,[12] few classes of rotaxanes have proved amenable to the construction of molecular shuttles. Still fewer shuttles operate using electrochemical stimuli, and two of these are among the only types of shuttle to be studied in any detail on surfaces. Willner and co-workers have characterized the shuttling kinetics of a cationic ring on a single-station rotaxane in which a cathode acts simultaneously as a redox reagent, a stopper, and a station.[7d,e] However, the integral role of the solid substrate in producing the bistability prevents comparisons with solution-phase experiments. An extensive program by Stoddart, Heath, and co-workers has studied the shuttling behavior of a particular class of redox-switched two-station shuttles in solid-state molecular electronic devices,[5] successfully correlating several aspects of their solution-phase, surface and solid-state behavior.[13]

We have previously reported[14] on another structural type of electrochemically switchable molecular shuttle; an amide-based[15−19] rotaxane in which net translocation of the macrocycle can be induced by photochemical or electrochemical reduction of a 1,8-naphthalimide station. The solution-phase shuttling was characterized in detail and both states were shown to exhibit unprecedented positional integrity. Furthermore, the shuttling motion is reversible and occurs over a rather large distance of ∼1.5 nm on a microsecond time scale (the precise rate is dependent on solvent and experimental conditions).[14] The relatively large, negative potentials required to cause switching, however, prevented the operation of such devices on surfaces.[20]

(5) (a) Mendes, P. M.; Flood, A. H.; Stoddart, J. F. *Appl. Phys. A* **2005**, *80*, 1197−1209. For a recent example, see: (b) Green, J. E.; Wook Choi, J.; Boukai, A.; Bunimovich, Y.; Johnston-Halperin, E.; DeIonno, E.; Luo, Y.; Sheriff, B. A.; Xu, K.; Shik Shin, Y.; Tseng, H.-R.; Stoddart, J. F.; Heath, J. R. *Nature* **2007**, *445*, 414−417.

(6) (a) Ichimura, K.; Oh, S. K.; Nakagawa, M. *Science* **2000**, *288*, 1624−1626. (b) Rosario, R.; Gust, D.; Garcia, A. A.; Hayes, M.; Taraci, J. L.; Clement, T.; Dailey, J. W.; Picraux, S. T. *J. Phys. Chem. B* **2004**, *108*, 12640−12642. (c) Braunschweig, A. B.; Northrop, B. H.; Stoddart, J. F. *J. Mater. Chem.* **2006**, *16*, 32−44. (d) Khuong, T. A. V.; Nunez, J. E.; Godinez, C. E.; Garcia-Garibay, M. A. *Acc. Chem. Res.* **2006**, *39*, 413−422. (e) Katsonis, N.; Kudernac, T.; Walko, M.; van der Molen, S. J.; van Wees, B. J.; Feringa, B. L. *Adv. Mater.* **2006**, *18*, 1397−1400. (f) Saha, S.; Leung, K. C. F.; Nguyen, T. D.; Stoddart, J. F.; Zink, J. I. *Adv. Funct. Mater.* **2007**, *17*, 685−693. (g) Willner, I.; Basnar, B.; Willner, B. *Adv. Funct. Mater.* **2007**, *17*, 702−717. (h) Vacek, J.; Michl, J. *Adv. Funct. Mater.* **2007**, *17*, 730−739. (i) Pollard, M. M.; Lubomska, M.; Rudolf, P.; Feringa, B. L. *Angew. Chem., Int. Ed.* **2007**, *46*, 1278−1280.

(7) (a) Willner, I.; Pardo-Yissar, V.; Katz, E.; Ranjit, K. T. *J. Electroanal. Chem.* **2001**, *497*, 172−177. (b) Sheeney-Haj-Ichia, L.; Willner, I. *J. Phys. Chem. B* **2002**, *106*, 13094−13097. (c) Katz, E.; Sheeney-Haj-Ichia, L.; Willner, I. *Angew. Chem., Int. Ed.* **2004**, *43*, 3292−3300. (d) Katz, E.; Lioubashevsky, O.; Willner, I. *J. Am. Chem. Soc.* **2004**, *126*, 15520−15532. (e) Katz, E.; Baron, R.; Willner, I.; Richke, N.; Levine, R. D. *ChemPhysChem* **2005**, *6*, 2179−2189. (f) Feng, M.; Gao, L.; Deng, Z.; Ji, W.; Guo, X.; Du, S.; Shi, D.; Zhang, D.; Zhu, D.; Gao, H. *J. Am. Chem. Soc.* **2007**, *129*, 2204−2205. (g) Guo, X. F.; Zhou, Y. C.; Feng, M.; Xu, Y.; Zhang, D. Q.; Gao, H. J.; Fan, Q. H.; Zhu, D. B. *Adv. Funct. Mater.* **2007**, *17*, 763−769. (h) Feng, M.; Gao, L.; Du, S. X.; Deng, Z. T.; Cheng, Z. H.; Ji, W.; Zhang, D. Q.; Guo, X. F.; Lin, X.; Chi, L. F.; Zhu, D. B.; Fuchs, H.; Gao, H. J. *Adv. Funct. Mater.* **2007**, *17*, 770−776.

(8) (a) Steuerman, D. W.; Tseng, H.-R.; Peters, A. J.; Flood, A. H.; Jeppesen, J. O.; Nielsen, K. A.; Stoddart, J. F.; Heath, J. R. *Angew. Chem., Int. Ed.* **2004**, *43*, 6486−6491. (b) Leigh, D. A.; Morales, M. A. F.; Pérez, E. M.; Wong, J. K. Y.; Saiz, C. G.; Slawin, A. M. Z.; Carmichael, A. J.; Haddleton, D. M.; Brouwer, A. M.; Buma, W. J.; Wurpel, G. W. H.; León, S.; Zerbetto, F. *Angew. Chem., Int. Ed.* **2005**, *44*, 3062−3067.

(9) Berná, J.; Leigh, D. A.; Lubomska, M.; Mendoza, S. M.; Pérez, E. M.; Rudolf, P.; Teobaldi, G.; Zerbetto, F. *Nat. Mater.* **2005**, *4*, 704−710.

(10) (a) Nguyen, T. D.; Tseng, H.-R.; Celestre, P. C.; Flood, A. H.; Liu, Y.; Stoddart, J. F.; Zink, J. I. *Proc. Natl. Acad. Sci. U.S.A.* **2005**, *102*, 10029−10034. (b) Nguyen, T. D.; Liu, Y.; Saha, S.; Leung, K. C.-F.; Stoddart, J. F.; Zink, J. I. *J. Am. Chem. Soc.* **2007**, *129*, 626−634.

(11) (a) Huang, T. J.; Brough, B.; Ho, C.-M.; Liu, Y.; Flood, A. H.; Bonvallet, P. A.; Tseng, H.-R.; Stoddart, J. F.; Baller, M.; Magonov, S. *Appl. Phys. Lett.* **2004**, *85*, 5391−5393. (b) Liu, Y.; Flood, A. H.; Bonvallet, P. A.; Vignon, S. A.; Northrop, B. H.; Tseng, H.-R.; Jeppesen, J. O.; Huang, T. J.; Brough, B.; Baller, M.; Magonov, S.; Solares, S. D.; Goddard, W. A.; Ho, C.-M.; Stoddart, J. F. *J. Am. Chem. Soc.* **2005**, *127*, 9745−9759.

(12) (a) Amabilino, D. B.; Stoddart, J. F. *Chem. Rev.* **1995**, *95*, 2725−2828. (b) Dietrich-Buchecker, C.; Rapenne, G.; Sauvage, J.-P. *Coord. Chem. Rev.* **1999**, *185−186*, 167−176. (c) Fujita, M. *Acc. Chem. Res.* **1999**, *32*, 53−61. (d) Raehm, L.; Hamilton, D. G.; Sanders, J. K. M. *Synlett* **2002**, 1742−1761. (e) Kim, K. *Chem. Soc. Rev.* **2002**, *31*, 96−107. (f) Kay, E. R.; Leigh, D. A. *Top. Curr. Chem.* **2005**, *262*, 133−177. (g) Bogdan, A.; Rudzevich, Y.; Vysotsky, M. O.; Böhmer, V. *Chem. Commun.* **2006**, 2941−2952. (h) Hutin, M.; Schalley, C. A.; Bernardinelli, G.; Nitschke, J. R. *Chem. Eur. J.* **2006**, *12*, 4069−4076. (i) Aucagne, V.; Hänni, K. D.; Leigh, D. A.; Lusby, P. J.; Walker, D. B. *J. Am. Chem. Soc.* **2006**, *128*, 2186−2187. (j) Wang, W.; Wang, L. Q.; Palmer, B. J.; Exarhos, G. J.; Li, A. D. Q. *J. Am. Chem. Soc.* **2006**, *128*, 11150−11159. (k) Vickers, M. S.; Beer, P. D. *Chem. Soc. Rev.* **2007**, *36*, 211−225. (l) Loeb, S. J. *Chem. Soc. Rev.* **2007**, *36*, 226−235. (m) Bäuerle, P.; Ammann, M.; Wilde, M.; Götz, G.; Mena-Osteritz, E.; Rang, A.; Schalley, C. A. *Angew. Chem., Int. Ed.* **2007**, *46*, 363−368. (n) Blight, B. A.; Wisner, J. A.; Jennings, M. C. *Angew. Chem., Int. Ed.* **2007**, *46*, 2835−2838. (o) Fuller, A.-M. L.; Leigh, D. A.; Lusby, P. J. *Angew. Chem., Int. Ed.* **2007**, *46*, 5015−5019. (p) Berná, J.; Crowley, J. D.; Goldup, S. M.; Hänni, K. D.; Lee, A.-L.; Leigh, D. A. *Angew. Chem., Int. Ed.* **2007**, *46*, 5709−5713. (q) Nygaard, S.; Laursen, B. W.; Hansen, T. S.; Bond, A. D.; Flood, A. H.; Jeppesen, J. O. *Angew. Chem., Int. Ed.* **2007**, *46*, 6093−6097. (r) Daniell, H. W.; Klotz, E. J. F.; Odell, B.; Claridge, T. D. W.; Anderson, H. L. *Angew. Chem., Int. Ed.* **2007**, *46*, 6845−6848.

(13) Choi, J. W.; Flood, A. H.; Steuerman, D. W.; Nygaard, S.; Braunschweig, A. B.; Moonen, N. N. P.; Laursen, B. W.; Luo, Y.; DeIonno, E.; Peters, A. J.; Jeppesen, J. O.; Xu, K.; Stoddart, J. F.; Heath, J. R. *Chem. Eur. J.* **2006**, *12*, 261−279.

(14) (a) Brouwer, A. M.; Frochot, C.; Gatti, F. G.; Leigh, D. A.; Mottier, L.; Paolucci, F.; Roffia, S.; Wurpel, G. W. H. *Science* **2001**, *291*, 2124−2128. (b) Altieri, A.; Gatti, F. G.; Kay, E. R.; Leigh, D. A.; Martel, D.; Paolucci, F.; Slawin, A. M. Z.; Wong, J. K. Y. *J. Am. Chem. Soc.* **2003**, *125*, 8644−8654.

(15) For other examples of photochemically responsive amide-based molecular shuttles, see ref 9 and: (a) Wurpel, G. W. H.; Brouwer, A. M.; van Stokkum, I. H. M.; Farran, A.; Leigh, D. A. *J. Am. Chem. Soc.* **2001**, *123*, 11327−11328. (b) Altieri, A.; Bottari, G.; Dehez, F.; Leigh, D. A.; Wong, J. K. Y.; Zerbetto, F. *Angew. Chem., Int. Ed.* **2003**, *42*, 2296−2300. (c) Bottari, G.; Leigh, D. A.; Pérez, E. M. *J. Am. Chem. Soc.* **2003**, *125*, 13360−13361. (d) Pérez, E. M.; Dryden, D. T. F.; Leigh, D. A.; Teobaldi, G.; Zerbetto, F. *J. Am. Chem. Soc.* **2004**, *126*, 12210−12211. (e) Li, Y.; Li, H.; Li, Y.; Liu, H.; Wang, S.; He, X.; Wang, N.; Zhu, D. *Org. Lett.* **2005**, *7*, 4835−4838. (f) Zhou, W.; Chen, D.; Li, J.; Xu, J.; Lv, J.; Liu, H.; Li, Y. *Org. Lett.* **2007**, *9*, 3929–3932.

(16) For an example of entropy-driven shuttling in an amide-based rotaxane, see: Bottari, G.; Dehez, F.; Leigh, D. A.; Nash, P. J.; Pérez, E. M.; Wong, J. K. Y.; Zerbetto, F. *Angew. Chem., Int. Ed.* **2003**, *42*, 5886−5889.

(17) For examples of chemically responsive amide-based molecular shuttles, see refs 3b, 8b and the following: (a) Da Ros, T.; Guldi, D. M.; Morales, A. F.; Leigh, D. A.; Prato, M.; Turco, R. *Org. Lett.* **2003**, *5*, 689−691. (b) Leigh, D. A.; Pérez, E. M. *Chem. Commun.* **2004**, 2262−2263. (c) Onagi, H.; Rebek, J., Jr. *Chem. Commun.* **2005**, 4604−4606. (d) Mateo-Alonso, A.; Fioravanti, G.; Marcaccio, M.; Paolucci, F.; Jagesar, D. C.; Brouwer, A. M.; Prato, M. *Org. Lett.* **2006**, *8*, 5173−5176. (e) Mateo-Alonso, A.; Ehli, C.; Aminur Rahman, G. M.; Guldi, D. M.; Fioravanti, G.; Marcaccio, M.; Paolucci, F.; Prato, M. *Angew. Chem., Int. Ed.* **2007**, *46*, 3521−3525. (f) Huang, Y.-L.; Hung, W.-C.; Lai, C.-C.; Liu, Y.-H.; Peng, S.-M.; Chiu, S.-H. *Angew. Chem., Int. Ed.* **2007**, *46*, 6629−6633.

(18) For examples of pH-responsive amide-based molecular shuttles, see: (a) Keaveney, C. M.; Leigh, D. A. *Angew. Chem., Int. Ed.* **2004**, *43*, 1222−1224. (b) Leigh, D. A.; Thomson, A. R. *Org. Lett.* **2006**, *8*, 5377−5379.

(19) For examples of transition metal-binding amide-based molecular shuttles, see: (a) Marlin, D. S.; Cabrera, D. G.; Leigh, D. A.; Slawin, A. M. Z. *Angew. Chem., Int. Ed.* **2006**, *45*, 77−83. (b) Marlin, D. S.; Cabrera, D. G.; Leigh, D. A.; Slawin, A. M. Z. *Angew. Chem., Int. Ed.* **2006**, *45*, 1385−1390.

(20) Cecchet, F.; Rudolf, P.; Rapino, S.; Margotti, M.; Paolucci, F.; Baggerman, J.; Brouwer, A. M.; Kay, E. R.; Wong, J. K. Y.; Leigh, D. A. *J. Phys. Chem. B* **2004**, *108*, 15192−15199.

Here, we report on a second member of this series, in which a naphthalene-1,4,5,8-diimide station can be switched between three different oxidation states. At each oxidation level, the naphthalene diimide exhibits a different binding affinity for the macrocycle, which leads to a different distribution of rings between two stations in a molecular shuttle. Conveniently, solution-phase cyclic voltammetry experiments allow the redox reactions to be carried out, the shuttling kinetics assessed, and the strongly biased co-conformational ratios quantified, all in the same experimental setup. The ratio of station occupancies can be altered over 6 orders of magnitude, from strongly favoring one station to strongly favoring the other, via an intermediate state in which the discrimination between the different binding sites is relatively modest. Furthermore, the switching conditions are sufficiently mild to allow access to two of the states when the rotaxanes are confined to an alkanethiol-based self-assembled monolayer (SAM) on gold. We report the characterization of molecular shuttle monolayers constructed through noncovalent interactions between the shuttle and the SAM. Unlike most previous examples of surface-confined shuttles, this arrangement results in alignment of the shuttle threads parallel to the substrate. Evidence for electrochemically controlled shuttling at a surface is demonstrated for the first time for the first time for a monolayer of amide-based molecular shuttles.

Design and Synthesis

In order to optimize the shuttling characteristics of the previously reported[14] shuttle **1a** (Chart 1), we investigated the effect of replacing the single imide group by a naphthalene-1,4,5,8-diimide. The more extensively delocalized aromatic system could be expected to have a less negative reduction potential for formation of the radical anion, but should also exhibit a second reduction process to give the dianionic state.[21] Simple AM1 calculations gave an indication of the charge density distribution in the neutral and reduced forms of the naphthalene monoimide and diimide (see Figure S1 in Supporting Information). In both cases, the extra electron density resulting from reduction is localized mainly on the electronegative oxygen atoms. As expected, adding one electron to the diimide system results in a smaller increase in electron density at each of the four oxygens compared to the effect of one additional electron on the two oxygens of the monoimide. The doubly reduced state of the diimide, however, exhibits a slightly higher charge density on the oxygens compared to the monoimide radical anion. Therefore, although a poor hydrogen-bond acceptor in the neutral state, reduction of the naphthalene diimide should increase the hydrogen-bond basicity of the oxygens (as previously demonstrated for 1,8-naphthalimide groups[14,22] and other imide systems[23,24]). Aromatic diimides have previously been used as neutral π-electron-poor templates for the formation of catenanes and rotaxanes.[25,26] Reduction of the diimide unit[25a,c] or addition of alkali metal salts[25b,c] have both been shown to disrupt the aromatic charge-transfer interactions and produce a co-conformational change in examples from this series but, to the best of our knowledge, the use of naphthalene diimide moieties as redox-switchable hydrogen-bond acceptors has not been investigated for the construction of molecular machines.[24]

Chart 1. Chemical Structures of Molecular Shuttles **1** and **2**, and Thread **3**[a]

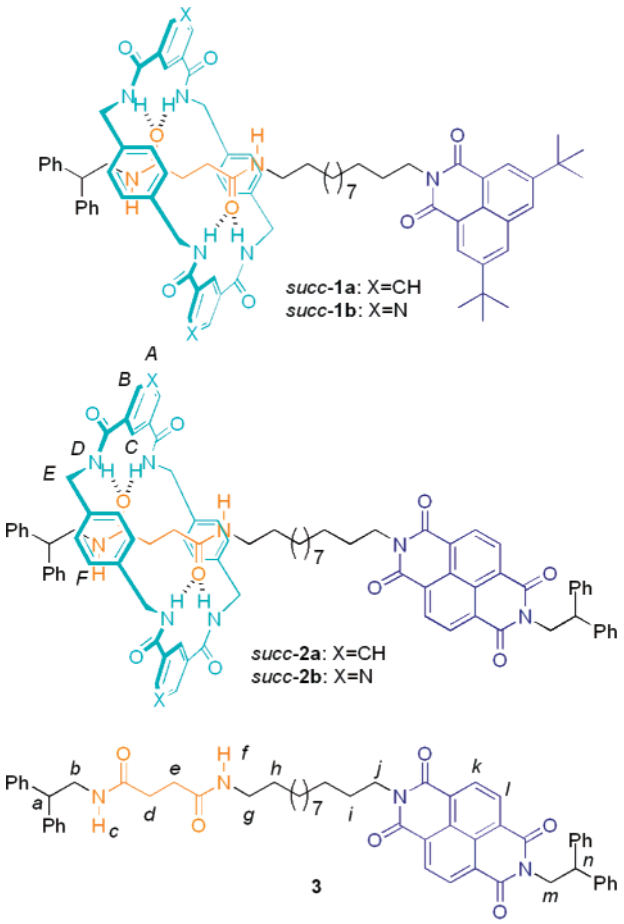

[a] Rotaxane structures are shown in the *succ*-co-conformation which is strongly preferred for the neutral molecules in all but the most polar of solvents (e.g., DMSO, formamide).[8b] Italicized lettering indicates non-equivalent proton environments.

In rotaxane **2** (Chart 1), a naphthalene-1,4,5,8-diimide (*ndi*)[27] station is separated from an electrochemically inert succinamide (*succ*) station by a C_{12} aliphatic spacer. The thread component

(21) Viehbeck, A.; Goldberg, M. J.; Kovac, C. A. *J. Electrochem. Soc.* **1990**, *137*, 1460−1466.
(22) (a) Ge, Y.; Lilienthal, R. R.; Smith, D. K. *J. Am. Chem. Soc.* **1996**, *118*, 3976−3977. (b) Niemz, A.; Rotello, V. M. *J. Am. Chem. Soc.* **1997**, *119*, 6833−6836. (c) Deans, R.; Niemz, A.; Breinlinger, E. C.; Rotello, V. M. *J. Am. Chem. Soc.* **1997**, *119*, 10863−10864. (d) Gray, M.; Cuello, A. O.; Cooke, G.; Rotello, V. M. *J. Am. Chem. Soc.* **2003**, *125*, 7882−7888.
(23) (a) Niemz, A.; Rotello, V. M. *Acc. Chem. Res.* **1999**, *32*, 44−52. (b) Carroll, J. B.; Gray, M.; McMenimen, K. A.; Hamilton, D. G.; Rotello, V. M. *Org. Lett.* **2003**, *5*, 3177−3180.
(24) In some supramolecular complexes where the oxidation state of an imide derivative has been used to control the binding constant, although hydrogen bonding to the imide carbonyls is involved, the overall association constant actually decreased on increasing imide charge as a consequence of stacking interactions with π-electron-rich aromatics. See: (a) Goodman, A.; Breinlinger, E.; Ober, M.; Rotello, V. M. *J. Am. Chem. Soc.* **2001**, *123*, 6213−6214. (b) Gray, M.; Goodman, A. J.; Carroll, J. B.; Bardon, K.; Markey, M.; Cooke, G.; Rotello, V. M. *Org. Lett.* **2004**, *6*, 385−388.
(25) See, for example: (a) Hamilton, D. G.; Montalti, M.; Prodi, L.; Fontani, M.; Zanello, P.; Sanders, J. K. M. *Chem. Eur. J.* **2000**, *6*, 608−617. (b) Vignon, S. A.; Jarrosson, T.; Iijima, T.; Tseng, H.-R.; Sanders, J. K. M.; Stoddart, J. F. *J. Am. Chem. Soc.* **2004**, *126*, 9884−9885. (c) Iijima, T.; Vignon, S. A.; Tseng, H.-R.; Jarrosson, T.; Sanders, J. K. M.; Marchioni, F.; Venturi, M.; Apostoli, E.; Balzani, V.; Stoddart, J. F. *Chem. Eur. J.* **2004**, *10*, 6375−6392, and references therein.
(26) Imides have also been used as fluorescent reporter units in rotaxane-based shuttles while playing no apparent role in interactions with the macrocycle. See, for example: Qu, D.-H.; Ji, F.-Y.; Wang, Q.-C.; Tian, H. *Adv. Mater.* **2006**, *18*, 2035−2038, and references therein.
(27) The nomenclature used to denote individual rotaxane states and isomers follows conventions adopted in previous papers (e.g., ref 14b). Namely, a bolded compound number refers to a given structural formula; the oxidation state is denoted by a superscript suffix (the absence of which indicates the neutral form); a prefix *succ* or *ndi* denotes the position of the macrocycle in a particular translational isomer.

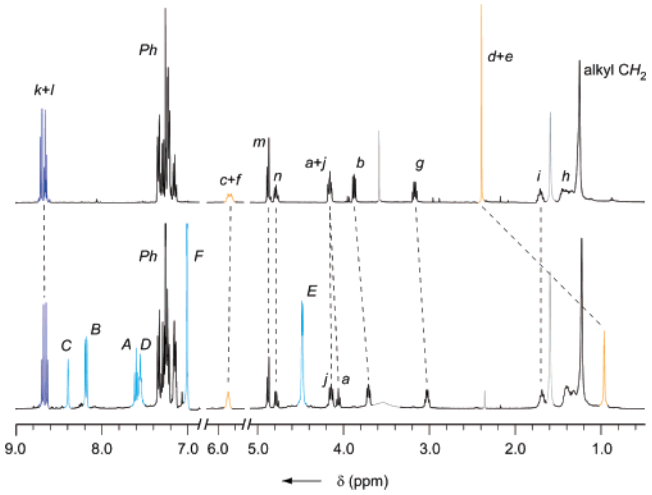

Figure 1. ^{1}H NMR spectra (400 MHz, $CDCl_3$, 298 K) of thread **3** (upper) and rotaxane **2a** (lower). The ^{1}H NMR assignments and coloring correspond to the labeling in Chart 1. Residual water peaks are shown in gray.

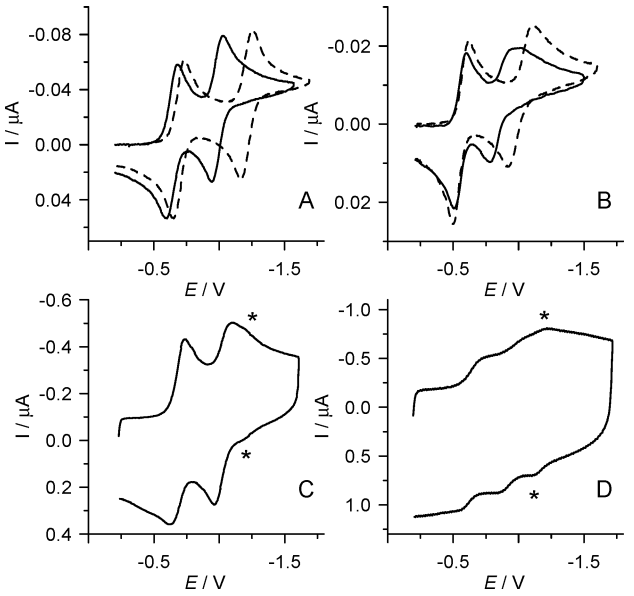

Figure 2. CV curves of a 0.5 mM solution of **2a** (solid lines) or **3** (broken lines) in THF (supporting electrolyte: 0.05 M tetrabutyl ammonium tetrafluoroborate). Working electrode: platinum disc (125 μm diameter). Potentials measured with respect to SCE. (A) $\upsilon = 1$ V s^{-1}, $T = 25$ °C; (B) $\upsilon = 1$ V s^{-1}, $T = -55$ °C; (C) $\upsilon = 100$ V s^{-1}, $T = 25$ °C; (D) $\upsilon = 1000$ V s^{-1}, $T = 25$ °C. Starred peaks (shoulders) indicate the presence of *succ*-**2a**$^{-\bullet/2-}$ intermediates as described in the text and Scheme 1.

bears two bulky diphenylethyl groups adjacent to each station in order to mechanically trap a benzylic amide macrocycle —a strong hydrogen-bond donor through the NH groups—onto the thread. The affinity of the succinamide station for this macrocycle is well established.[14] Rotaxane **2a** bears an isophthalamide-derived macrocycle, which is replaced by the analogous pyridine-3,5-dicarboxamide cycle in **2b**. This change does not significantly affect the macrocycle−thread interactions, but is required for the surface immobilization of the shuttles (vide infra). The rotaxanes were each obtained in a five-component clipping reaction starting from thread **3**. Full synthetic details are provided in the Supporting Information.

Co-Conformation in the Neutral State. Comparing the ^{1}H NMR spectrum of **2a** in $CDCl_3$ with that of the thread molecule **3** (Figure 1) confirms that the preferred co-conformation of the rotaxane in solution is *succ*-**2a** (as shown in Chart 1). In particular, the succinamide methylene protons (H_d and H_e in Chart 1 and Figure 1) show an upfield shift of $\Delta\delta = -1.43$ ppm in the rotaxane compared to the thread, characteristic of shielding caused by aromatic ring currents in the *p*-xylylene rings of the macrocycle. Smaller shifts are also observed for the protons flanking the *succ* station (H_a, H_b, and H_g). Conversely, no shifts can be distinguished for any other protons in the thread, including those of the naphthalene diimide, indicating that the macrocycle resides almost exclusively over the succinamide station. A similar situation is observed with rotaxane **2b** (see Figure S2 of the Supporting Information).

Redox-Switched Shuttling. The dynamics of the electrochemically induced shuttling in **2a** were studied in detail using cyclic voltammetry (CV) at various scan rates (υ) and temperatures (Figure 2). At 298 K and $\upsilon \leq 50$ V s^{-1} (Figure 2A), the voltammogram of **2a** in THF (Bu_4NBF_4 as supporting electrolyte) displays two reversible peaks associated with the consecutive reductions of the *ndi* station.[21] Compared to the CV of the thread (**3**) both redox processes are shifted to less negative potentials, and the positive shift is notably larger in the case of the second reduction than the first (compare $E_{1/2} = -0.64$ and -0.98 V for **2a**, and -0.68 and -1.21 V for **3**). Consistent with the electrostatic nature of hydrogen bonding, the observed changes in the CV pattern of **2a** reflect the stabilization of the mono and dianion of the *ndi* station as a consequence of their increasing ability to form hydrogen bonds with the macrocycle.[14b,22,23] Previously, we have shown that, in **1a**,[14b] such stabilization occurs due to shuttling of the macrocycle from the succinamide station (*succ*-**2a** co-conformer), where it is preferentially located in the neutral state, onto the (reduced) *ndi* station (*ndi*-**2a**$^{-\bullet/2-}$ co-conformer).[28]

The response of the CV curves to changing scan rate and temperature (Figure 2, parts B−D) is also consistent with electrochemically induced shuttling. As the temperature is lowered and/or the scan rate increased, the shuttling process becomes slow on the time scale of the experiment. This is illustrated in Figure 2, parts C and D, by the presence of cathodic and anodic shoulders (denoted by asterisks) associated with processes involving the un-shuttled *succ*-**2a** co-conformation. Furthermore, the broadening of the second reduction peak at low temperature (Figure 2B) also indicates the presence of both co-conformers in the diffusion layer.

Further evidence for shuttling was obtained by performing wider CV scans so as to induce reduction of the macrocycle (Figure S3 of the Supporting Information). Because of the fast and irreversible protonation of isophthaloyl-based dianions,[29] the amide groups in the reduced macrocycle can no longer form hydrogen bonds with the thread, so that the features of the reverse scan resemble the reoxidation of thread **3**—there is now no interaction between the macrocycle and the reduced *ndi* station.

The CV data can be fully rationalized by considering the extended square scheme (ladder) mechanism set out in Scheme

(28) When a group that is too bulky for the macrocycle to pass over was placed in between the two stations in **1**, the CV of the rotaxane mirrored that of the corresponding thread; i.e., the shift in the redox potential in the rotaxane must arise from shuttling of the macrocycle to the reduced station. See ref 14b.

(29) Ceroni, P.; Leigh, D. A.; Mottier, L.; Paolucci, F.; Roffia, S.; Tetard, D.; Zerbetto, F. *J. Phys. Chem. B* **1999**, *103*, 10171−10179.

Scheme 1. Extended Square Scheme (Ladder Mechanism) for the Redox-Switched Operation of Molecular Shuttle **2a**[a]

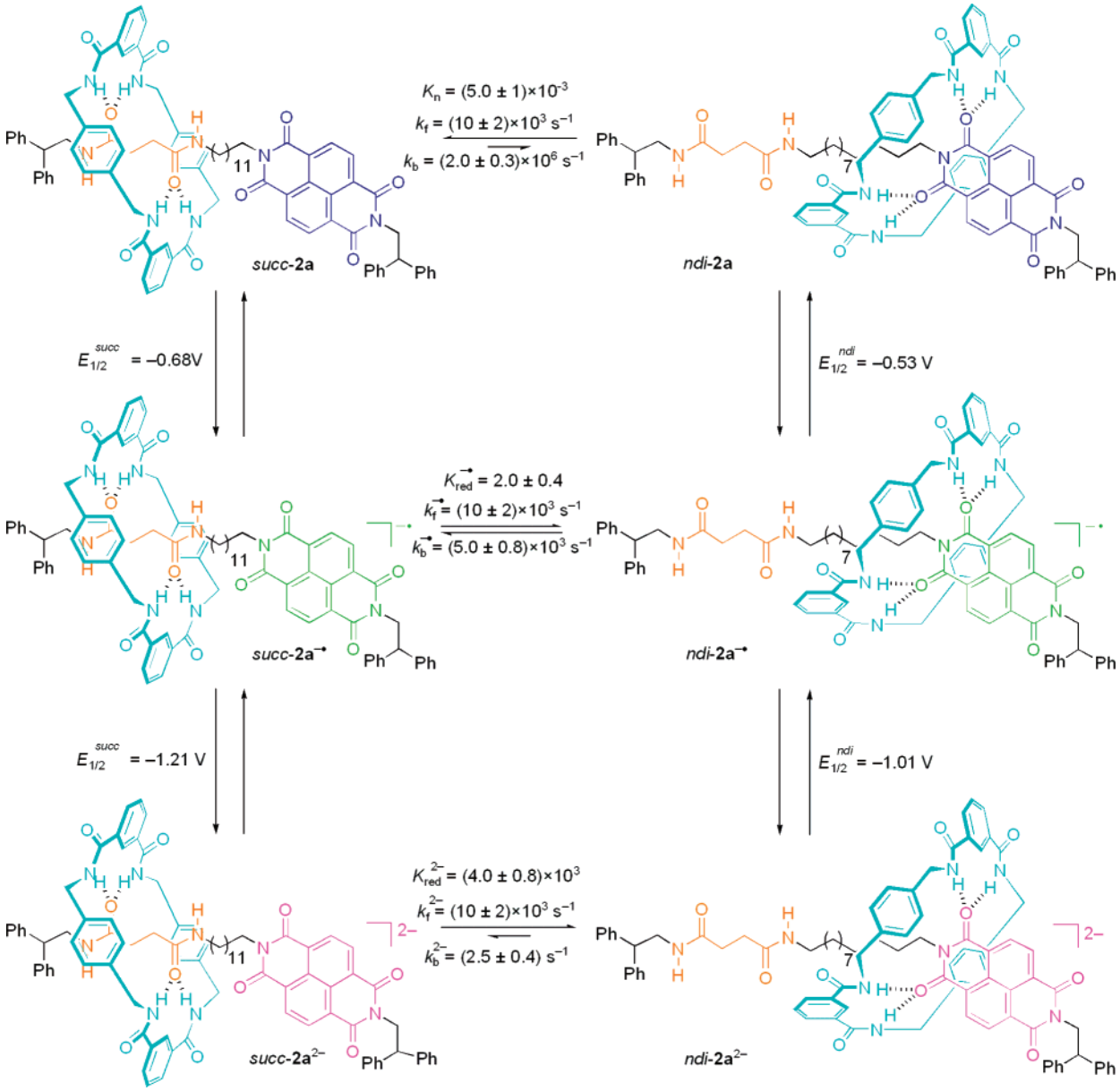

[a] Electrochemical reactions are shown as vertical transitions and co-conformational equilibria in each oxidation state as horizontal 'rungs'. Thermodynamic and kinetic parameters shown here were calculated by simulation and fitting of the CV curves obtained in THF (supporting electrolyte: 0.05 M tetrabutylammonium tetrafluoroborate); working electrode: platinum disc (125 μm diameter); $T = 25$ °C.

1.[30] The six chemical species are interrelated by a series of heterogeneous electron-transfer reactions (vertical transitions) and homogeneous translational isomerizations (horizontal transitions). Under the conditions of Figure 2A (i.e., relatively slow scan rates and high temperatures), the two different co-conformations both contribute to a single reversible voltammetric peak for each redox reaction, with an apparent $E_{1/2}$ value that is related to the true value for the individual translational isomers and the equilibrium constant for their interconversion.[31] Alternatively, when experimental conditions are chosen so that the chemical intermediates cannot reach their equilibrium concentrations (as a consequence, for instance, of reducing the time scale of the experiment or decreasing the temperature, Figure 2, parts B−D), a less reversible CV pattern is observed and features associated with each individual co-conformation become visible in the curve.[31] The shape and position of the CV curves is therefore very sensitive to the relative values of the thermodynamic and kinetic constants for the different homogeneous and heterogeneous equilibria shown in Scheme 1, as well as the experimental conditions. The parameters may be calculated by fitting the shape and the position of the voltammetric peaks using digital simulation techniques.[31,32] The CV curves in Figure 2 were successfully reproduced (Figure S5 of the Supporting Information) using the relevant kinetic and thermodynamic parameters reported in Scheme 1 and Table S1 (see the Supporting Information).

(30) Evans, D. H. *Chem. Rev.* **1990**, *90*, 739−751.
(31) Lerke, S. A.; Evans, D. H;. Feldberg, S. W. *J. Electroanal. Chem.* **1990**, *296*, 299−315.
(32) Bard, A. J.; Faulkner, L. R. *Electrochemical Methods*; Wiley: New York, 2001.
(33) Chatterjee, M. N.; Kay, E. R.; Leigh, D. A. *J. Am. Chem. Soc.* **2006**, *128*, 4058−4073.

As observed by ^{1}H NMR (vide supra), the *succ*-**2a** co-conformation dominates in the neutral state ($K_n = (5.0 \pm 1) \times 10^{-3}$). Reduction to the radical anion **2a**$^{-\bullet}$ increases the hydrogen-bond basicity of the *ndi* station such that the equilibrium ratio of co-conformers is now $K_{red}^{-\bullet} = 2.0 \pm 0.4$. The poorer discrimination between the two stations compared to that observed for the radical anion of **1a** (ref 14b) is consistent with the greater delocalization in the larger diimide system and the AM1 results (see Figure S1 of the Supporting Information). However, a second reduction gives the dianionic state **2a**$^{2-}$ where the hydrogen-bonding ability of the *ndi* unit is further increased to the extent that the *ndi*-**2a**$^{2-}$ co-conformation is now strongly preferred ($K_{red}^{2-} = (4.0 \pm 0.8) \times 10^3$).

The reduction potentials for the *succ*-**2a** co-conformations were set identical to those of the thread **3** during the simulation process, whereas it can be seen that when the macrocycle is on the *ndi* station, both redox processes occur at less negative potentials due to stabilization of the reduced species by the electron-withdrawing effect of forming hydrogen bonds through the imide carbonyls. The "forward" shuttling (*succ* → *ndi*) rates (k_f) in all states were assumed to be the same ($k_f = k_f^{-\bullet} = k_f^{2-} = (10 \pm 2) \times 10^3$ s^{-1}) and similar to the value previously determined for $k_f^{-\bullet}$ in **1a** under the same conditions.[14b] This is consistent with a shuttling mechanism in which the rate-determining step is cleavage of the noncovalent interactions between the macrocycle and the electrochemically inert *succ* station, with little or no involvement of the *ndi* station, irrespective of its oxidation state. The increased stability of the *ndi* co-conformation with increasing charge is reflected in the decreasing "backward" shuttling (*ndi* → *succ*) rates (k_b), as obtained by the simulations.

The same experiments performed on **2b** revealed quantitatively identical behavior (within the accuracy of the simulation procedure, see Figure S4 and Table S1 of the Supporting Information). In both of these shuttles, therefore, controlling the redox state of the *ndi* station changes the strength of hydrogen bonds between the *ndi* unit and the macrocycle so that the equilibrium constant between the two co-conformations (i.e., the average position of the macrocycle on the thread) can be effectively modulated over 6 orders of magnitude in two, roughly evenly spaced, intervals (Figure 3). Rotaxane **2** represents the first molecular shuttle in which the affinity of one station for the macrocycle can be varied between three well-defined states using a single external stimulus.

Molecular Shuttle Monolayers. With the aim of achieving redox-induced shuttling in a molecular monolayer, the electrochemical addressability of **2b** attached to a conducting surface was investigated. The majority of studies on immobilized molecular shuttles to date have involved the attachment of a rotaxane thread to surfaces or incorporation into a polymeric matrix.[5−8,10,34,35] Recently, however, we have investigated the attachment of the macrocycle of the rotaxane to a surface as an alternative approach to creating functional shuttle-based devices.[9,20,36] In this procedure, pyridine groups in the macrocycle are used to attach the rotaxane to a self-assembled monolayer (SAM) of 11-mercaptoundecanoic acid (11-MUA) by forming hydrogen bonds with the 11-MUA carboxylates. The relatively minor structural modification required to incorporate the pyridine moiety, together with the simple deposition procedure,

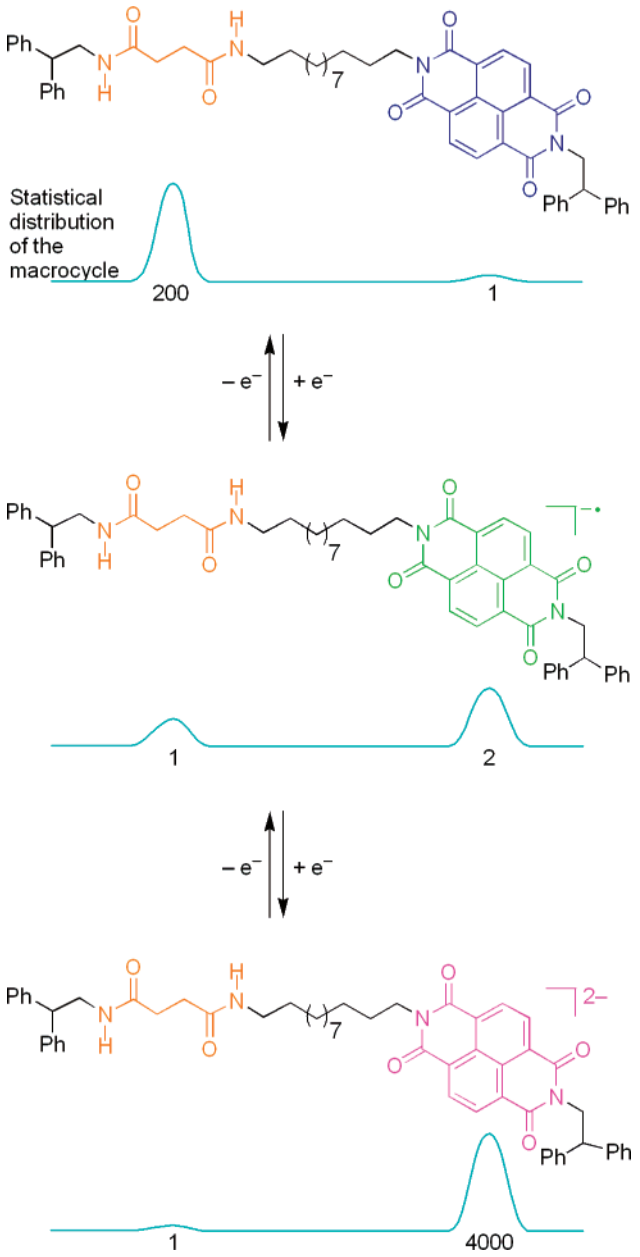

Figure 3. Machine-performance representation[33] of electrochemically switchable three-state molecular shuttle **2a** in THF (supporting electrolyte: 0.05 M tetrabutylammonium tetrafluoroborate); working electrode: platinum disc (125 μm diameter); T = 25 °C. The population trace shows the statistical distribution in the relative position of the macrocycle with respect to the thread.

(34) Investigation of molecular-level motions in drop-casted, vacuum-evaporated or spin-coated thin films or polycrystalline samples of catenanes and rotaxanes is another emerging area of interest. See, for example: (a) Cavallini, M.; Biscarini, F.; León, S.; Zerbetto, F.; Bottari, G.; Leigh, D. A. *Science* **2003**, *299*, 531−531. (b) Moulin, J. F.; Kengne, J. C.; Kshirsagar, R.; Cavallini, M.; Biscarini, F.; Leon, S.; Zerbetto, F.; Bottari, G.; Leigh, D. A. *J. Am. Chem. Soc.* **2006**, *128*, 526−532. (c) Biscarini, F.; Cavallini, M.; Kshirsagar, R.; Bottari, G.; Leigh, D. A.; Leon, S.; Zerbetto, F. *Proc. Natl. Acad. Sci. U.S.A.* **2006**, *103*, 17650−17654. (d) Farrell, A. A.; Kay, E. R.; Bottari, G.; Leigh, D. A.; Jarvis, S. P. *Appl. Surf. Sci.* **2007**, *253*, 6090−6095.

(35) Polyrotaxane architectures also allow preparation of solid-state interlocked species. For examples of electroactive polyrotaxanes, see: (a) Zhu, S. S.; Carroll, P. J.; Swager, T. M. *J. Am. Chem. Soc.* **1996**, *118*, 8713−8714. (b) Zhu, S. S.; Swager, T. M. *J. Am. Chem. Soc.* **1997**, *119*, 12568−12577. (c) Buey, J.; Swager, T. M. *Angew. Chem., Int. Ed.* **2000**, *39*, 608−612. (d) Kwan, P. H.; Swager, T. M. *Chem. Commun.* **2005**, 5211−5213.

(36) Cecchet, F.; Pilling, M.; Hevesi, L.; Schergna, S.; Wong, J. K. Y.; Clarkson, G. J.; Leigh, D. A.; Rudolf, P. *J. Phys. Chem. B* **2003**, *107*, 10863−10872.

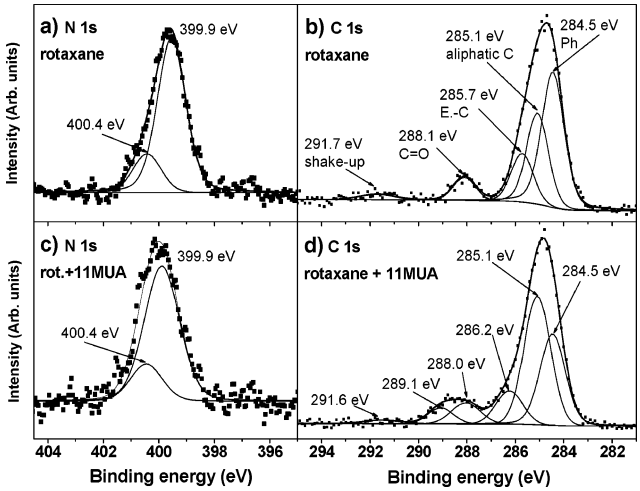

Figure 4. X-ray photoemission spectra of N 1s (a; c) and C 1s (b; d) core levels of rotaxane **2b** deposited on gold (a; b) and grafted onto 11-MUA SAM (c; d). Spectra (a) and (b) were collected with resolution 1.0 eV, while (c) and (d) were collected with resolution 1.2 eV. Raw data (■) and fit to the experimental line (—) are shown.

makes this a particularly convenient method for anchoring molecular structures to surfaces.

Rotaxane **2b** was grafted to the surface of a monolayer of 11-MUA self-assembled on a gold electrode, according to the previously employed procedure.[9,20,36] The resulting **2b**·11-MUA·Au films were characterized by X-ray photoelectron spectroscopy (XPS). Rotaxane **2b** and 11-MUA molecules present X-ray photoemission signals that can overlap, such as the different components in the C 1s core level signal. We therefore initially analyzed a reference sample of **2b** directly deposited on gold to identify all of the characteristic spectral features of the rotaxane molecule before carrying out measurements on the **2b**·11-MUA·Au sample.

Figure 4a shows the N 1s core level photoemission spectrum of rotaxane **2b** on gold, which is composed of a main peak at 399.9 eV, resulting from the amide and pyridine groups, and a shoulder at 400.4 eV, which corresponds to the nitrogen atoms of the imide groups. The relative area of the two components is in agreement with the stoichiometry of the rotaxane. Exactly the same features can be seen in Figure 4c which shows the N 1s spectral region of **2b**·11-MUA·Au—clear proof that the functionalization of the SAM with the rotaxane was successful.

The C 1s core level spectrum of rotaxane **2b** on gold (Figure 4b) contains contributions from carbon atoms in several different chemical environments. In practice, XPS may not distinguish between all the various types of carbon, and therefore, the standard fitting procedure consists of reconstructing the spectrum with a minimum number of peaks consistent with the raw data, the experimental resolution and the molecular structure, with carbon atoms under very similar chemical environments (i.e., very close in binding energy) considered equivalent and represented by a single peak. Following this criterion, the C 1s spectrum in Figure 4b was fitted by five peaks. The component at 284.5 eV can be unambiguously assigned to aromatic carbons and is associated with the $\pi-\pi^*$ shakeup structure at 291.7 eV that represents 5% of the aromatic signal.[37] The peak at 285.1 eV is due to aliphatic carbons, while the one at 285.7 eV represents carbon atoms bound to electronegative atoms. Finally, the well-defined peak at 288.1 eV is the signature of carbonyl groups.[38] Each of these peaks from **2b** directly on gold are also present in the C 1s spectrum of **2b**·11-MUA·Au (Figure 4d). However, there are also new features arising from 11-MUA. In particular, the peak at 285.1 eV in Figure 4d is more intense than the corresponding signal in Figure 4b, as a consequence of the contribution from 11-MUA alkyl-chain carbons, while the intensity and position of the component at 286.2 eV, which represents carbon atoms attached to electronegative atoms, is also influenced by the contribution of 11-MUA and interactions between the rotaxane and 11-MUA SAM. The signal at 289.1 eV originates from carboxylic acid groups.[39]

Quantitative analysis of the XPS spectra allows us to determine the amount of C, N, O, and S on the surface (hydrogen is not detected by XPS). The coverage (the proportion of 11-MUA carboxylic groups that are functionalized with rotaxanes) can be estimated by comparing the experimentally determined atomic percentages, derived from the intensity of the photoemission line, with those calculated from the stoichiometry of the molecules at various surface coverages. For the calculation, we considered a model surface of 100 alkanethiol chains functionalized with two, six or ten rotaxane molecules, corresponding to a functionalization yield of 2, 6, or 10%. Table S2 of the Supporting Information presents the experimental and theoretical results obtained. The signal of electrons coming from atoms closer to the Au substrate is attenuated more than the signal from the topmost layer. Therefore, in the quantification procedure we corrected the intensity of the S 2p area taking into account the attenuation[40] experienced by electrons traveling though an ~17 Å layer thickness and assuming that the attenuation is only due to the presence of 11-MUA.[41] The experimental values are in good agreement with a coverage of 6%. Additionally, it should be noted that carbon and especially oxygen signals always contain a contribution of atmospheric contaminants, which affects all percentages.

This apparently small number of rotaxane-derivatized carboxylates results from the orientation adopted by the molecular shuttles and actually corresponds to virtually complete coverage of the SAM surface area. The rationale for this is, as previously shown for **1b**·11-MUA·Au,[20] the macrocycle is anchored perpendicular to the surface with the thread parallel to the surface plane such that each rotaxane molecule occupies a large surface area.

Redox-Switched Shuttling on a Surface. A different amide-based molecular shuttle (which switches on the basis of alkene photoisomerization) has previously been grafted onto a SAM of 11-MUA in a similar fashion, creating surfaces which exhibit switchable wettability and across which a liquid droplet may be transported on application of the shuttling stimulus.[9] Direct observation of the rotaxane shuttling motion on the surface, however, has yet to be achieved. Reversible shuttling obviously

(37) Beamson, G.; Briggs, D. *High Resolution XPS of Organic Polymers: The Scienta ESCA300 Database*; John Wiley & Sons: Chichester, 1992.

(38) (a) Whelan, C. M.; Cecchet, F.; Clarkson, G. J.; Leigh, D. A.; Caudano, R.; Rudolf, P. *Surf. Sci.* **2001**, *474*, 71−80. (b) Mendoza, S. M.; Whelan, C. M.; Jalkanen, J.-P.; Zerbetto, F.; Gatti, F. G.; Kay, E. R.; Leigh, D. A.; Lubomska, M.; Rudolf, P. *J. Chem. Phys.* **2005**, *123*, 244708.

(39) Mendoza, S. M.; Arfaoui, I. E.; Zanarini, S.; Paolucci, F.; Rudolf, P. *Langmuir* **2007**, *23*, 582−588.

(40) (a) Bain, C. D.; Whitesides, G. M. *J. Phys. Chem.* **1989**, *93*, 1670−1673. (b) Laibinis, P. E.; Bain, C. D.; Whitesides, G. M. *J. Phys. Chem.* **1991**, *95*, 7017−7021.

(41) (a) Porter, M. D.; Bright, T. B.; Allara, D. L.; Chidsey, C. E. D. *J. Am. Chem. Soc.* **1987**, *109*, 3559−3568. (b) Bindu, V.; Pradeep, T. *Vacuum* **1998**, *49*, 63−66.

requires the surface itself to be stable to the stimulus employed. Unfortunately, relatively large negative potentials are incompatible with gold–thiolate SAMs, which are unstable at potentials below ca. −1.0 V.[42] This prevented study of electrochemical shuttling in previously constructed films of **1b**·11-MUA·Au,[20] but we reasoned that the less negative first reduction potential of the naphthalene diimide redox center in **2b** could allow access to at least the monoanion, and consequently electrochemically induced shuttling in the monolayer.

Electrochemical Impedance Spectroscopy (EIS) and double-potential step chronoamperometry (CA) were used to investigate the reduction of **2b**·11-MUA·Au. Typically, both bare and rotaxane-modified SAMs possessed rather low double-layer capacitance values. Furthermore, in both cases, the film capacitance was nearly independent of the applied potential, thus excluding any significant rearrangement of the 11-MUA SAM structure upon the application of potential. Additionally, in the case of **2b**·11-MUA·Au, the EIS spectra (Figure S6 of the Supporting Information) displayed the typical potential-dependent semicircle associated with slow electron transfer (ET) processes that would involve the *ndi* station. Simulation and fitting of the EIS spectra obtained at various potentials allowed calculation of the relevant parameters associated with the electronic response of the interface. In particular, a value of $\sim 10^3\ s^{-1}$ was obtained for the heterogeneous ET rate constant. Such a low value, together with the rather small time constant of the electrode ($\sim 8\ \mu s$, also obtained by fitting of the EIS data), permitted investigation of the heterogeneous ET kinetics to and from immobilized **2b** by double potential step chronoamperometry.[43]

In such experiments, the electrode potential is stepped back and forth between two limiting values while the current is monitored continuously during the experiment. The potential switching frequency is chosen so as to fit with the time scale of the relevant electrochemical process.[32] An example of two subsequent CA experiments is shown in Figure 5A. At very short times, double-layer charging dominates the current decay while, at relatively longer timescales, faradaic currents involving reduction or oxidation of the redox centers on the surface are observed. By choosing initial and final potential levels that correspond to the fully oxidized and monoanion reduced states of the immobilized species, respectively, information concerning the dynamics of the ET processes is obtained from the exponential decay of the CA currents.[43] In particular, if significant rearrangements or chemical modifications take place in the film following the ET event, such as the shuttling of the

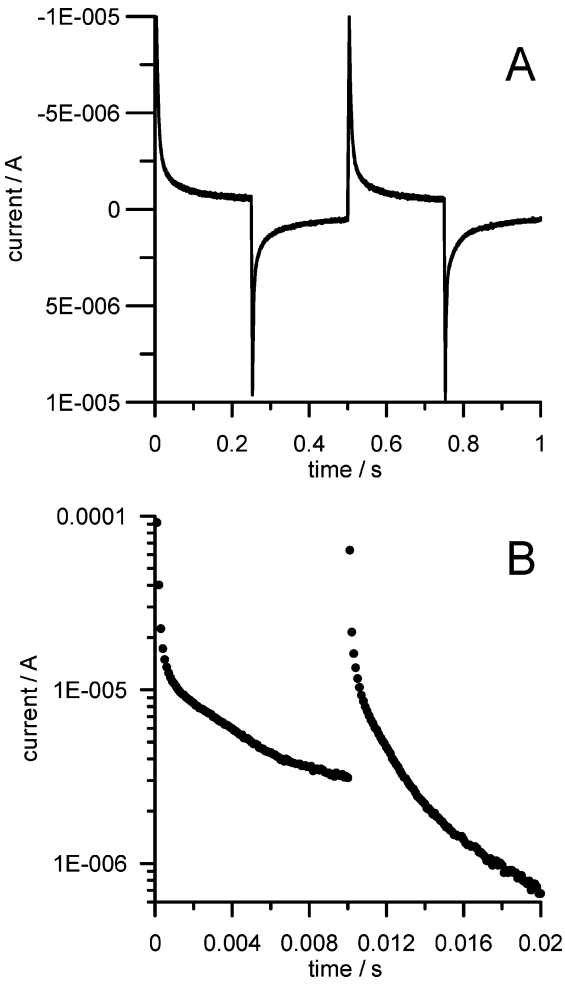

Figure 5. CA transients recorded for the SAM **2b**·11-MUA·Au. (A) Forward step potential: −0.4 V; backward step and initial potential: 0 V; step duration: 0.25 s. (B) Forward step potential: −0.9 V; backward step and initial potential: 0 V; step duration: 10 ms. Solution: aqueous 0.1 M KCl, $T = 25$ °C. For the sake of comparison, in (B) absolute values of the current are displayed.

macrocycle along the thread, then the backward and forward current transients will be non-symmetrical. Electron transfer involving adsorbed redox species through non-defective SAMs occurs via non-resonant through-bond tunneling (i.e., the rate decreases exponentially with the chain length) with decay constants ranging from 0.8−1.5 $Å^{-1}$ for saturated chains to 0.2−0.6 $Å^{-1}$ for unsaturated ones.[44] Any factor affecting the electronic coupling between an attached redox moiety and the electrode (e.g., the number and type of covalent bonds, bond conformations, noncovalent interactions, direct versus through-bond coupling) causes the ET rate to change markedly. Double potential step CA has proven to be a sensitive method for detecting the existence of structurally different binding modes of redox moieties to electrodes and to detect electrochemically induced phenomena on films such as bending or translocation of redox-active units tethered to the electrode.[6g] Recently, CA was successfully used to follow the electrochemically induced motion of a threaded cyclophane along a molecular string associated with the electrodes.[7d,e]

The CA transients recorded for **2b**·11-MUA·Au when the potential was stepped between 0 V and −0.4 V (i.e., remaining

(42) In alkaline aqueous systems, this has been shown to be the result of partial reversible reductive desorption of the thiolates. The exact potential at which this occurs varies with certain structural features, and consequently this process has been widely studied as a method for probing the molecular structure of monolayers. See, for example: (a) Widrig, C. A.; Chung, C.; Porter, M. D. *J. Electroanal. Chem.* **1991**, *310*, 335−359. (b) Walczak, M. M.; Popenoe, D. D.; Deinhammer, R. S.; Lamp, B. D.; Chung, C. K.; Porter, M. D. *Langmuir* **1991**, *7*, 2687−2693. (c) Kakiuchi, T.; Usui, H.; Hobara, D.; Yamamoto, M. *Langmuir* **2002**, *18*, 5231−5238. Even under neutral conditions, or in organic solvents where reductive desorption is not observed within the solvent window, alkanethiolate SAMs are still destroyed at negative potentials. The details of this complex, kinetically controlled, process are less well understood. See, for example: (d) Everett, W. R.; Welch, T. L.; Reed, L.; Fritsch-Faules, I. *Anal. Chem.* **1995**, *67*, 292−298. (e) Everett, W. R.; Fritsch-Faules, I. *Anal. Chim. Acta* **1995**, *307*, 253−268. (f) Beulen, M. W. J.; Kastenberg, M. I.; van Veggel, F.; Reinhoudt, D. N. *Langmuir* **1998**, *14*, 7463−7467. See also: (g) Finklea, H. O. In *Electroanalytical Chemistry*; Bard, A. J., Ed.; Marcel Dekker: New York, 1996; Vol. 19, p 109.

(43) Chidsey, C. E. D. *Science* **1991**, *251*, 919−922.

(44) Paddon-Row, M. N. In *Stimulating Concepts in Chemistry*; Vögtle, F.; Stoddart, J. F.; Shibasaki, M., Eds.; Wiley-VCH: Weinheim, 2000; pp. 267−292.

more positive than the reduction potential of **2b**, Figure 5A) show symmetric backward and forward transients indicating that no structural change occurs under these conditions. Non-symmetric backward-to-forward transients were, however, observed when the potential was stepped from 0 V (corresponding to neutral **2b**) to −0.9 V (sufficiently negative to reduce the *ndi* stations), and then back to 0 V (Figure 5B). All transients, recorded during either the forward or the backward steps, displayed a short-lived (<0.1 ms) component associated with double-layer charging in agreement with the very small time constant of the electrode. A slower component (with $\tau \approx$ 3 ms) was then observed in both transients, compatible with the reduction (in the forward step) and reoxidation (in the backward one) of the *ndi* station. A rate constant of ∼300 s^{-1} is in fact typical of ET processes involving redox probes immobilized onto the surface of SAMs formed from alkanethiols with alkyl chains of 12−14 methylene units.[45]

A third component with an intermediate time scale of ∼0.2 ms was also observed in the backward step but not the forward step. Once the double-layer charging current was subtracted, this component amounted to ∼2/3 of the overall current decay. This is an indication that the injection of electrons to the *ndi* station of **2b** and their subsequent removal occurs along different molecular pathways. The co-conformational changes associated with the shuttling process that follows the reduction of the *ndi* station in solution would explain the ET behavior of immobilized rotaxanes: in the *succ*-**2b** co-conformation (i.e., during the forward step), the shortest way for electrons to get from the electrode surface to the redox site (*ndi*) is via weak interactions between the diimide carbonyls and the terminal carboxylate groups of the SAM. Such a process would correspond to the ∼3 ms component of the transients. Upon reduction, however, the rotaxane undergoes shuttling that would make the redox-active station more efficiently electronically wired (via hydrogen bonds) to the macrocycle and therefore with the SAM, generating the faster transient (∼0.2 ms) observed in the oxidation step. In fact, unbound reduced (negatively charged) *ndi* stations should be repelled from the SAM surface, which carries a negative charge under the experimental conditions (pH 7).[46] So, in the absence of a shuttling process, it might be expected that the reoxidation of the *ndi* station would be a slower process than reduction. The experimentally observed 10-fold acceleration of the ET rate for the oxidation step is equivalent to shortening of the alkane bridge by two methylene units.[47] The high reproducibility of the CA transients in subsequent experiments suggests that, following reoxidation, backward shuttling of the macrocycle to restore the *succ*-**2b** co-conformation is efficient. Simulations of the shuttling mechanism in the monolayer were performed (Figure S8 of the Supporting Information) and suggest that the equilibrium concentrations of the two co-conformations would in fact be reached on the surface within the 10 ms reduction step. This explains the presence, in the backward transient, of both slow and fast components. The fact that the fast transient, corresponding to oxidation of *ndi*-$\mathbf{2b}^{-\bullet}$·11-MUA·Au(111), accounts for ∼2/3 of the overall decay is in-line with the solution-phase results (Figure 3) where a 1:2 *succ*-$\mathbf{2a}^{-\bullet}$:*ndi*-$\mathbf{2a}^{-\bullet}$ co-conformational ratio was observed.

Conclusions

Perhaps the best way to appreciate the technological potential of controlled molecular-level motion is to recognize that molecular-level machines lie at the heart of every significant biological process. Nature has not repeatedly chosen this solution for achieving complex task performance without good reason. In terms of artificial molecular machines, electrochemistry is a particularly attractive operating stimulus from the viewpoint of integration with current technologies and also allows for a powerful set of analytical tools to characterize the molecular-level motion across a range of different environments. In this second generation of redox-active imide molecular shuttles, the positional discrimination and rapid shuttling kinetics of the original system have been improved upon in a shuttle that now exhibits three distinct macrocycle distributions, all accessible using only electrochemistry. Crucially from the perspective of future applications, the electrochemically induced shuttling between two of these states has been demonstrated for a SAM of amide-based molecular shuttles for the first time. The shuttling is fast (millisecond time scale), reversible, and the kinetics and thermodynamics can be probed with a range of experimental techniques. These systems represent a significant new addition to the few classes of artificial molecular machines that have been shown to operate on surfaces to date.

Acknowledgment. This work was supported by the European Union Future and Emerging Technology program Hy3M, the University of Bologna, the Italian MIUR, The Netherlands Organization for the Advancement of Research (NWO) and the Carnegie Trust for the Universities of Scotland. D.A.L. is an EPSRC Senior Research Fellow and holds a Royal Society-Wolfson Research Merit Award.

Supporting Information Available: Synthetic procedures and spectroscopic data for rotaxanes **2a** and **2b**. AM1 calculations of imide and diimide charge densities. Details of CV simulation parameters, supplementary CV experiments and EIS experiments. Details of monolayer preparation and characterization. This material is available free of charge via the Internet at http://pubs.acs.org.

JA077223A

(45) Smalley, J. F.; Feldberg, S. W.; Chidsey, C. E. D.; Linford, M. R.; Newton, M. D.; Liu, Y.-P. *J. Phys. Chem.* **1995**, *99*, 13141−13149.
(46) (a) Molinero, V.; Calvo, E. J. *J. Electroanal. Chem.* **1998**, *445*, 17−25. (b) Azzaroni, O.; Vela, M. E.; Martin, H.; Creus, A. H.; Andreasen, G.; Salvarezza, R. C. *Langmuir* **2001**, *17*, 6647−6654.
(47) Becka, A. M.; Miller, C. J. *J. Phys. Chem.* **1992**, *96*, 2657−2668.